Solid Freeform Fabrication 2024: Proceedings of the 35th Annual International Solid Freeform Fabrication Symposium – An Additive Manufacturing Conference
Reviewed Paper

Multi-Nozzle Cooperation for Micro-Cold Spray

Ronnie F. P. Stone*, Michael Gammage†, Junmin Wang*, Michael Cullinan*, Desiderio Kovar*, Zhenghui Sha* [1]

* Walker Department of Mechanical Engineering, The University of Texas at Austin, TX 78712

† DEVCOM Army Research Lab

Abstract

While the multi-robot systems (MRS) paradigm has successfully emerged in fused deposition modeling (FDM) processes for cooperative 3D printing, one of its core goals is the development of a framework that is adaptable to different forms of additive manufacturing (AM) technologies. Of particular interest to MRS are processes that benefit from multi-material and multi-resolution capabilities and face inherent scalability issues. Micro-cold spray (MCS) has been historically limited to systems with single-nozzle configurations, which restrict the range of viable printing applications. A multi-nozzle, MRS-inspired configuration may allow independent control of deposition parameters and feature sizes. In this paper, we develop a computational MRS framework as the first step in enabling multi-nozzle cooperation for MCS and demonstrate it using a dual-nozzle example. Specifically, we focus on rules for slicing, motion planning, and process scheduling.

Keywords: Cooperative Additive Manufacturing, Micro-Cold Spray, Multi-Robot Systems.

1. Introduction

Since the introduction of robotic systems in manufacturing, numerous processes, such as assembly and production of electronic components, have experienced significant improvements in speed, reliability, and efficiency [1]. Beyond extending existing robot capabilities, such as the repeatability, speed, and reachability (workspace volume) of manipulators, researchers have explored the potential of adding more robots to collaborate on larger-scale and more complex tasks, for instance, the handling of heavy and flexible objects [2]. This shift in research focus is recognized as the multi-robot systems (MRS) paradigm. While it may be intuitive to expect a positive correlation between the number of robots involved in a task and the associated manufacturing speed, MRS introduces several technical challenges that need to be addressed. For instance, although MRS enables cooperation, it requires meticulous planning for collision-free operations. This added complexity hinders the application of MRS in many manufacturing contexts, particularly those without inherent scalability issues, such as subtractive manufacturing, where the marginal benefit of adding more robots is small.

In contrast, additive manufacturing (AM) processes have been benefited significantly from adopting the MRS approach, typically by integrating multiple deposition tools or end-effectors within a shared workspace. Many AM technologies are notoriously plagued by poor scalability in both size and speed, limiting their industrial applications. Therefore, the development of an MRS-based AM framework holds promise in resolving some existing challenges in AM processes, provided that the inherent complexities of MRS can be efficiently managed.

Micro-cold spray (MCS) is an emerging AM technology traditionally limited to single-nozzle

[1]Corresponding author: zsha@austin.utexas.edu

configurations and primarily used to deposit thick films [3]. Unlike traditional cold spray techniques, MCS does not necessitate thermally regulated substrates and is capable of depositing brittle materials to near full density [4], significantly broadening its range of applications. However, MCS requires specific process conditions, such as pressure and particle size, to achieve satisfactory deposition performance, which involves reaching a material-specific impact velocity [5]. These stringent requirements hinder the flexibility of a single-nozzle configuration, as seamlessly varying the parameters during the manufacturing process becomes infeasible. Therefore, following recent research efforts in adapting AM processes to the MRS paradigm, we propose a multi-nozzle MCS system framework. This system aims to allow for independent control of deposition parameters and feature sizes, potentially overcoming the limitations of single-nozzle configurations and enhancing the flexibility and scalability of MCS technology.

In this paper, we particularly focus on a dual-nozzle system where each nozzle has a distinct throat diameter, thus allowing for different printing resolutions. We also explore how the proposed system can be used to create 3D features, extending beyond thick films, a feat not yet achieved in MCS. By 3D features in MCS, we mean parts with arbitrarily-many layers above the first anchoring layer of the material with the substrate, just like in FDM printing. Furthermore, to the best of the authors' knowledge, there are no existing multi-nozzle systems for MCS. Therefore, the key contribution of this paper is the computational framework for such a system and its potential applications. Although we focus on the design of a dual-nozzle system, our overall system design and computational framework can be extended to multi-nozzle systems.

The remainder of the paper is structured as follows. Section 2 discusses the related work available in the literature, specifically concerning MRS in AM processes and the challenges associated with MCS. Section 3 outlines the conceptual framework and the scope of the problem. Our methodology is presented in Section 4. Section 5 describes our preliminary numerical results, and Section 6 details future research directions.

2. Related Work

While the extension of traditional MCS systems to use multiple nozzles has not yet been explored, other AM processes have successfully adapted to the MRS paradigm. In the realm of FDM printing, numerous cooperative multi-nozzle systems have been developed (see [6] for a systematic review). These systems use multiple nozzles to increase both the speed and the build volume of the process. In terms of hardware, such systems can take the form of fixed manipulators [7], gantry systems [8], or mobile robots [9]. However, designing a cooperative multi-nozzle MCS system presents unique challenges due to its underlying physics, particularly because of the necessary flow conditions for deposition and strict environment requirements. MCS requires a vacuum-sealed deposition environment [10], making the use of large manipulators and mobile robots infeasible for small-scale deposition chambers typical in existing systems. Hence, the MRS configuration most likely to be adaptable to MCS is gantry-based.

Cooperative gantry systems are divided into two types: multi-gantry and multi-nozzle. Multi-gantry systems have each nozzle connected to a separate moving platform, giving the entire system $3n$ degrees of freedom (where n is the number of nozzles) and allowing independent control of each nozzle [11]. On the other hand, multi-nozzle systems mount all extruders to a single gantry, spatially coupling them [12]. For true cooperative printing, the multi-gantry system is preferred as it provides

the system with more degrees of freedom to cooperate, including greater flexibility for synchronous operation. Multi-gantry systems have been widely used in fast construction applications [13] and standard polymer printing [14], achieving significant reductions in manufacturing time compared to single-gantry systems.

Regardless of the hardware configuration of the cooperative system, one of the incentives for adapting AM processes to the MRS paradigm is to efficiently print large 3D features. The printing of such features is still largely unexplored in MCS, as the underlying physics inherently hinders the smooth accumulation of deposited material. In attempts to increase the thickness of films and create 3D features, researchers have studied the effects on surface roughness when performing multiple scans on a given area [15]. Although different research groups use various metrics to characterize film roughness, it is generally observed that roughness correlates positively with the number of scans [16], which can potentially make the creation of large, non-homogeneous 3D features prohibitive. The causes of cratering are not well understood, but it has been suggested that it could be due to differences in particle size [17] or preferential deposition caused by the geometric heterogeneity of the anchoring layer [18]. This increase in roughness is not material-specific, as it has been observed in a range of particle and substrate combinations [19, 20]. Therefore, our goal is to start filling this knowledge gap by laying the computational and theoretical foundations necessary for designing multi-nozzle MCS systems that can be used for multi-resolution applications and, consequently, for the creation of 3D features.

3. System Description

A multi-nozzle MCS system introduces new operational challenges, requiring fundamental design modifications in both software and hardware compared to the single-nozzle system. Before determining the necessary design changes and the associated computational framework, we must clearly define how the system should function, as a multi-nozzle MCS system may operate differently depending on the desired manufacturing application.

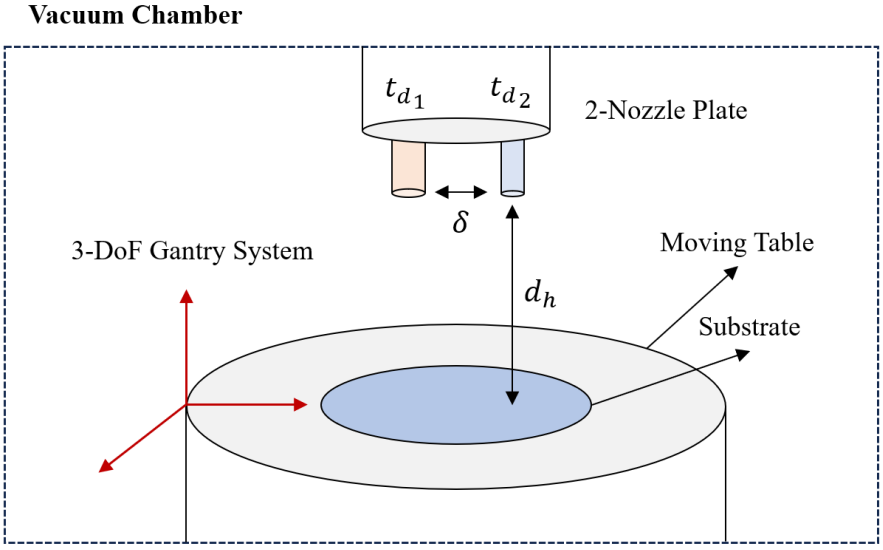

Figure 1: Overview of the design of the deposition area for the dual-nozzle MCS system.

In this paper, we focus on a dual-nozzle MCS system where each nozzle has a distinct throat diameter t_{d_n}, allowing for different printing (deposition) resolutions. The choice of a dual-nozzle system is purely for ease of demonstration and eventual hardware setup, as the framework does not lose generality and can be applied to n-nozzle systems. As previously discussed, a mobile or manipulator-based system would be impractical in MCS, which is generally confined to small-scale vacuum chambers. Therefore, we choose a system design in which the nozzles are fixed, positioned a small distance δ apart, and the table holding the substrate is moved using a 3-DoF gantry system (Fig. 1). This approach eliminates the need for complex collision-free motion planning typical of MRS, as only the table can move, making nozzle-to-nozzle collisions impossible. The only constraint that must be taken into account is that the distance from the tip of the nozzle to the substrate, denoted the deposition height d_h, must be within a certain range for optimal deposition, which depends on the material being used and the throat diameter t_{d_n}.

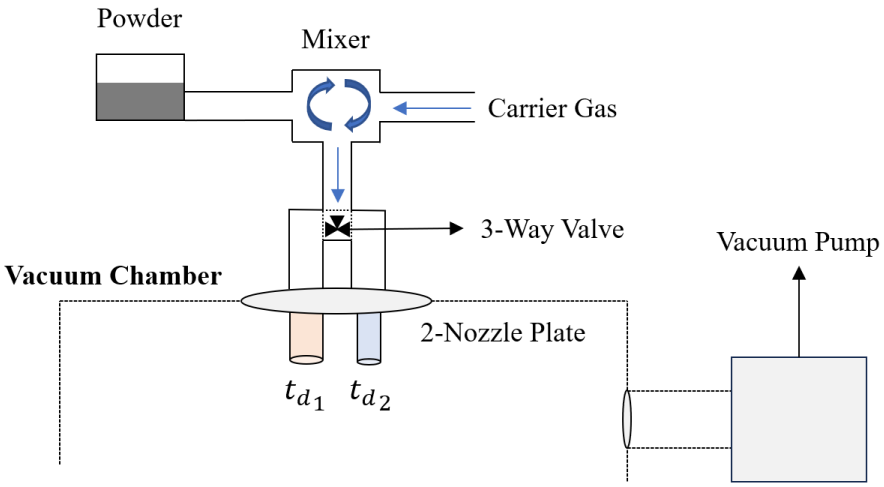

Figure 2: Overview of the gas and aerosol flow for the dual-nozzle MCS system.

The main downside of using fixed nozzles is that the system loses cooperability when operating both nozzles simultaneously, as they are spatially coupled. This means that synchronous operation can only produce deposition paths separated by δ. However, while simultaneous use of both nozzles is possible, we limit our scope to asynchronous nozzle operation for several practical reasons. Synchronous multi-nozzle systems would generally require independent gas control for each nozzle, significantly increasing hardware cost and required physical space. Additionally, if the nozzles had more degrees of freedom, which would be the natural reason to have synchronous operation, they could rotate in directions perpendicular to the supersonic flow, potentially altering flow dynamics and affecting the deposition density [21, 22]. Therefore, both nozzles in our proposed system are connected to the same flow pipe through a 3-way valve. When one nozzle is operational, the other one receives no flow due to the valve. This approach allows the mechanical design of the remainder of the system to remain virtually identical to a single-nozzle configuration (Fig. 2).

Finally, since we are interested in taking advantage of the dual-nozzle MCS system to build 3D features, we need to make assumptions about the deposition profile. In the remainder of the paper,

we assume that the deposition profile is Gaussian [23]. This means that if we look at the cross-section of any deposited line (viewing parallel to the line), we would expect to see accumulated material in the shape of a scaled normal distribution with a specified height. Since there are two different nozzles, each has its own deposition profile. For instance, the profile f for any nozzle could be defined as:

$$f = h \exp\left(\frac{x^2}{2\sigma^2}\right), \; h = \frac{A}{\sigma\sqrt{2\pi}}, \tag{1}$$

where A is a scaling factor and σ is the standard deviation of the deposition profile. Note that we adopt standard Gaussian, i.e., the mean μ of the distribution is set to 0, since mathematically we are only concerned with the shape of the function. The scaling factor is added since we do not want to restrict the function to have a specific height or area under the curve, since those can vary when depositing using nozzles with different throat diameters (Fig. 3).

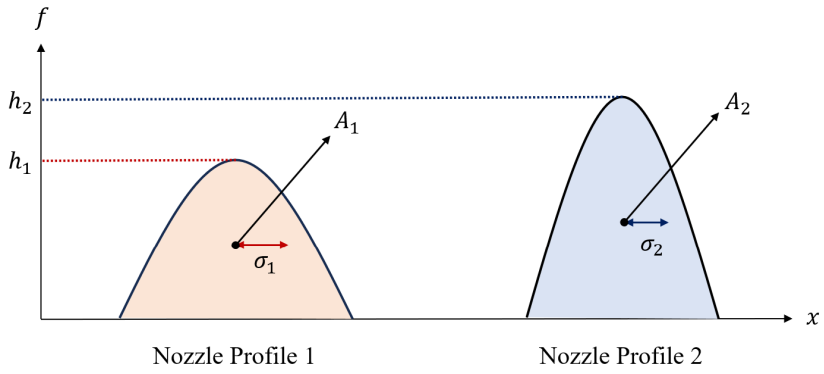

Figure 3: Nozzles with different throat diameters may have different, albeit always Gaussian, deposition profiles depending on the process parameters.

4. Methodology

Now that the base hardware design has been defined, we present the proposed computational framework. The first challenge we must address is how to perform move actions without depositing material onto the substrate. Unlike FDM printing and other AM processes, where it is possible to simply retract the material, the flow in MCS cannot stop instantaneously. To address this, we propose a shutter system that can cover both nozzles (since we cannot determine a priori which nozzle is active) when a move command is given. As long as the duration of the move commands is minimized—a common optimization goal in most AM raster patterns—the accumulation of material on the shutter should not be a concern. From a computational framework perspective, every move command should then be preceded by an activate shutter command and followed by a deactivate shutter command once the target location is reached (Fig. 4). The flow parameters remain constant during the movement, preserving the steady-state flow condition throughout and allowing the deposition to continue normally as soon as the shutter is opened. Note that when we say that the nozzle moves to a certain position, in reality, the table moves such that the desired position is under the desired nozzle. However, in this paper, we use both expressions interchangeably.

The next technical challenge that must be addressed is the switch of nozzles during the printing process. Since both nozzles share the same gas control and the start and stop of the flow are

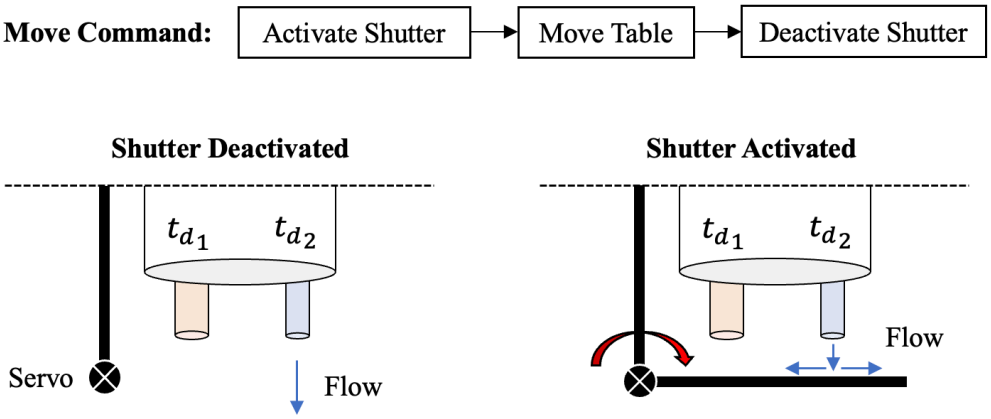

Figure 4: Overview of the shutter design to enable move command.

not instantaneous, taking time to reach a steady state, a specified transition time (t_s) is necessary. Simply using the shutter system is not sufficient, as t_s might be on the order of minutes while the flow parameters are adjusted to accommodate the new throat diameter. Therefore, we propose establishing a dumping region in which the material can be deposited away from the substrate while the shutter is deactivated.

When a nozzle switch command is given, a move command is issued such that the nozzle is positioned at the closest point of the dumping region, utilizing the shutter to prevent unintended substrate deposition. Then, the flow gradually transitions between both nozzles through the valve until the desired active nozzle reaches steady state and is ready for deposition. As the transition occurs, another move command is issued to move the nozzle along the dumping region to another point that is closest to its next destination, thus shortening the future travel distance when the transition is finished. Note that if the move command occurs entirely within the dumping region, the shutter is not activated as it is not needed. Finally, once the nozzle transition is complete, a move command is given and the table moves to position the next printing location under the nozzle. This sequence of commands minimizes the time that the shutter needs to be active, adhering to our principle of minimizing move commands outside the dumping region (Fig. 5).

With the two new commands, "move" and "switch", the dual-nozzle MCS system can complete any printing task. However, in general, the user should aim to provide a G-code that, for each layer, does all the printing moves of one nozzle, and then all the printing moves of the other nozzle, reducing the amount of nozzle switches.

4.1. Creating 3D Features (Ideal Case)

One of the key challenges in creating 3D features with MCS is that the surface of the layers tends to become rougher as the number of scans increases because of the Gaussian-like deposition profile. This effect can be exacerbated by repeated scanning locations in the same position, creating increasingly higher peaks and progressively lower valleys. We approach this problem by considering a new scanning strategy that attempts to smooth out the deposition layer. We start by considering a single-nozzle system which has a deposition profile f. Instead of using a traditional raster scan, typical of FDM systems, we deposit lines separated by a small distance, denoted the

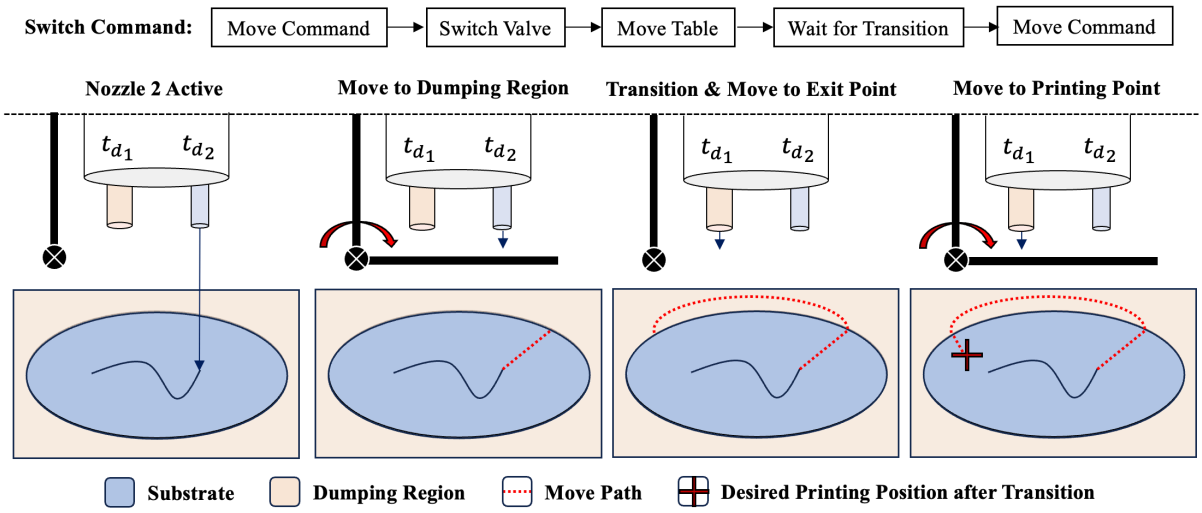

Figure 5: Overview of the sequence of commands to switch the operating nozzle.

separation parameter ϵ. Once those initial lines are deposited, a second pass is performed in between them to fill the gaps. The key idea is that we would be able to fill those gaps with exactly the amount of area missing and build a layer with a smooth surface (Fig. 6).

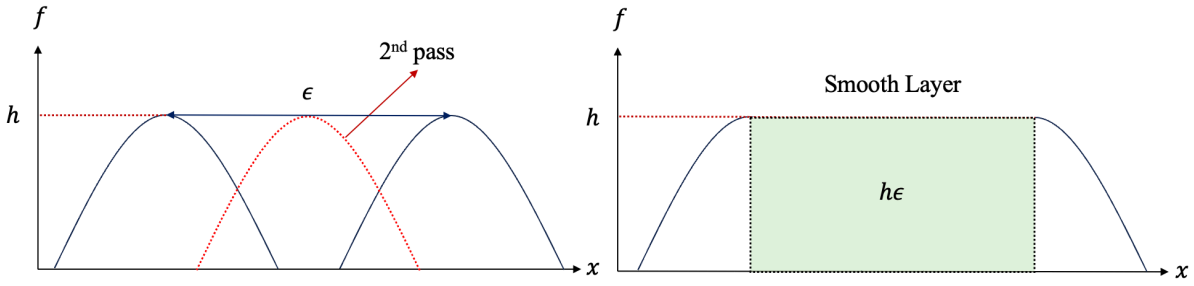

Figure 6: New scanning strategy for MCS that allows for the creation of smoother layers.

However, the question we have to answer is, how far apart the first lines should be, that is, what is a good value for ϵ? If we assume that the deposition parameters remain constant during the process, which would be ideal from an operational perspective, each pass always deposits the same amount of material. Since the Gaussian profile is symmetric along the x- and y-axis, we can abstract the problem to say that the lines always have the same cross-sectional area. Therefore, if the goal is to fill the gap, we have to find ϵ such that the area of the gap is exactly the area of the deposition profile. Naturally, this assumes that the deposition behaves in a sand-like manner, filling the gap sequentially from the bottom to the top. It is nonetheless the best we can do in this scanning strategy when only using one nozzle.

The area gap A_g is simply the difference between the square formed by h and ϵ and A (Fig. 6), where A is the area of the Gaussian, as previously defined:

$$A_g = h\epsilon - A. \tag{2}$$

Since we are constraining the gap area to be equal to the deposition area, we can replace h according to its definition in Eq. 1, and solve for ϵ:

$$\epsilon = 2\sigma\sqrt{2\pi}. \tag{3}$$

Therefore, the optimal ϵ can be found analytically, and depends only on the standard deviation of the deposition profile.

Now, if we consider the dual-nozzle system, we note that we have more options regarding the scanning strategy. The first obvious difference is that it is now possible to fill the middle gaps with the smaller nozzle instead. Therefore, the separation parameter ϵ can be re-computed such that the gap area is equal to the deposition area of the smaller nozzle. Following the same procedure as before, we have:

$$\epsilon = (\frac{A_2}{A_1} + 1)\sigma_1\sqrt{2\pi}, \tag{4}$$

which reduces to Eq. 3 if $A_2 = A_1$. Hence, the optimal separation parameter ϵ is a function of the standard deviation of the deposition profile of the larger nozzle and the ratio of the deposition areas of the smaller nozzle to the larger one.

4.2. Creating 3D Features (Non-Ideal Case)

So far we have assumed that if the gap area is exactly equal to the deposition area of the nozzle filling the gap, then the layer surface would smooth out completely. In reality, that may not happen due to the underlying physics of the process. A likely more realistic assumption would be that the middle layers are also Gaussian. Therefore, we assume that the middle layer creates another Gaussian peak that is exactly the same height as the adjacent layers. This can be done by carefully tuning the deposition parameters (Fig. 7).

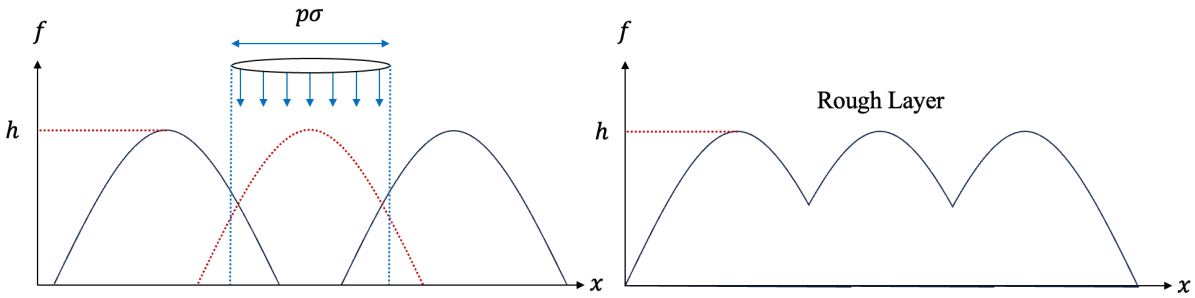

Figure 7: Due to the underlying physics, the middle row deposition may create a rough surface layer instead.

For such a situation to be physically possible, the deposition of the middle layer must not interfere with the peaks of the adjacent layers. Therefore, before discussing this scenario, we must first define how the nozzle operates. We do that by assuming that the nozzle diameter is related to the standard deviation of its associated Gaussian deposition profile. Specifically:

$$t_d = p\sigma, \tag{5}$$

where σ is the standard deviation of the profile and p is a positive integer that defines the range of direct flow deposition. The key idea here is that the actual deposition is done on top of the segment $p\sigma$ but may grow larger and therefore become thinner (more Gaussian-like) in the extremities due to the physics of the process.

The next point to recognize is that as we increase the number of passes, the layer becomes flatter. This is because every new pass divides the peak-to-peak distance by exactly $\epsilon/2$. Therefore, the flatness of the layer in this model can be defined as

$$f_{lt} = \epsilon 2^{-m}. \tag{6}$$

This process, again, shows the benefits of having a multi-nozzle MCS system to realize multi-resolution print for 3D feature creation. However, due to the possible nozzle interference described by Eq. 5, we cannot indefinitely do any number of passes. Therefore, we can frame the problem of choosing the number of passes m and the separation parameter ϵ as a constrained optimization problem:

$$\begin{aligned} \min \quad & \epsilon \\ \text{s.t.} \quad & \epsilon > 2^m p \sigma_2 \\ & \epsilon < \epsilon_{max}, \end{aligned} \tag{7}$$

where σ_2 is the standard deviation of the smaller nozzle deposition profile. The parameters p and m are the same as previously defined. The rationale behind minimizing ϵ is that theoretically the flatness of the layer should increase due to Eq. 6. The first constraint relates to the fact that the flow coming directly from the nozzle cannot interfere with the adjacent Gaussian peaks, as determined by Eq. 5, and it has a natural exponential nature to it as the desired number of passes increases. The second constraint puts a limit on how large ϵ is allowed to be and is, in a sense, a desired minimum printing resolution. Hence, using this framework, one would be able to find the optimal ϵ depending on the choice of importance between flatness and printing resolution.

5. Numerical Results

We performed several numerical simulations of what the optimal ϵ should be depending on the choice of parameters. For $p = 6$, $\sigma_2 = 0.1$, $\epsilon_{max} = 2.5$, we get the following table by varying the desired number of passes m:

Number of Passes	ϵ (mm)	f_{lt} (mm)
1	1.2	0.6
2	2.4	0.6
3	2.5	-

Table 1: Optimal separation parameter and associated flatness as a function of the number of passes.

What we notice from Tb. 1 is that the flatness value remains constant regardless of the number of passes, if we find the optimal ϵ. Therefore, the flatness will always vary with regards to the parameters p and σ_2 but not with the desired number of passes. Note that, for the previous case, once the number of passes reaches 3, the optimal ϵ goes beyond the constraint, and therefore is not a valid solution.

Number of Passes	ϵ (mm)	f_{lt} (mm)
1	0.5	0.25
2	1.0	0.25
3	2.0	0.25
4	4.0	-

Table 2: Optimal separation parameter with different set of parameters.

For a different choice of $p = 5$, $\sigma = 0.05$, and $\epsilon_{max} = 2.5$ we get similar results:

Furthermore, we graphically simulated what a typical sliced layer would look like, for a variety of different geometries, when attempting to build such 3D features and using the optimization framework presented, as shown in Figure 8.

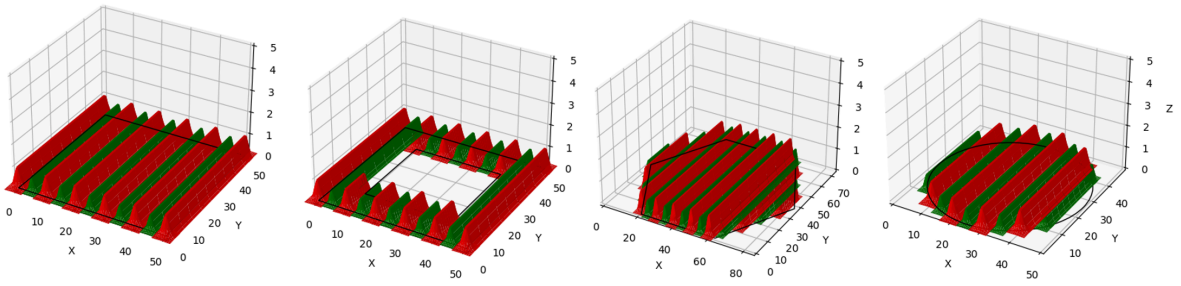

Figure 8: Due to the underlying physics, the middle row deposition may create a rough surface layer instead.

The results, albeit preliminary, show that the framework is able to deal with a complex geometries, and can take the estimated flatness of the top of the created layer into consideration when slicing. Additionally, it clearly shows the dependency of the flatness and resolution values on the choice of parameters, which can further guide the design of the dual-nozzle MCS system, particularly in the design of throat diameter ratios and deposition profile.

6. Discussion

While the proposed system and associated framework are promising, there are many areas of our research that require further exploration. The first aspect that we want to explore is having an accurate model of what the deposition profile (i.e., the parameter σ) looks like. This will require controlled testing to see how the deposition parameters, such as nozzle speed and feed rate, can affect the profile (e.g., whether the shape would be Gaussian-like or not, and the correlation between deposition parameters and distribution parameters) and whether it is consistent throughout the manufacturing process. If the profile cannot be kept consistent, then our methodology for building 3D features would have to be modified to account for such process uncertainties.

Another aspect we will consider in future work is optimizing the scanning pattern to minimize movement time. Unlike other MRS-based AM processes, minimizing the total time of move commands is crucial for our dual-nozzle MCS system, since it relies on a shutter-based mechanism. For now, as shown in the results, we use a traditional zig-zag scanning pattern, which simplifies

slicing and motion planning but can produce long move commands. Naively, considering the other extreme, which could be the Hilbert-curve pattern, may have a negative impact on the methodology of creating 3D features since it relies on accurately filling the gaps between adjacent lines.

Finally, we want to be able to experimentally quantify the surface roughness when using our novel scanning strategy to build 3D features. Specifically, we would like to be able to define a roughness metric and see how it changes as the number of layers scanned increases. This metric would come directly from physical measurements and would not rely on the wide range of assumptions made throughout the methodology section.

7. Conclusions

To conclude, in this paper we designed the first ever dual-nozzle MCS system and the computational framework necessary for its operation. Compared to the single-nozzle variant, we made significant changes to the physical design to allow moving and nozzle-switching commands. Additionally, we established simple heuristic-driven rules for slicing and motion planning to minimize manufacturing time. Finally, we studied the concept of how two nozzles with different resolutions can facilitate the printing of large 3D features by producing layers with decreased roughness. We look forward to exploring the new research directions outlined in the Discussion section.

Acknowledgement

The authors thank the Army Research Lab for supporting this work via grant number W911NF-24-2-0007. We would also like to acknowledge helpful conversations with Stephen Bierschenk and Matthew Na for his assistance with plotting the sliced layers.

References

[1] A. Gasparetto, L. Scalera, *et al.*, "A brief history of industrial robotics in the 20th century," *Advances in Historical Studies*, vol. 8, pp. 24–35, 2019.

[2] F. Caccavale and M. Uchiyama, "Cooperative manipulation," *Springer handbook of robotics*, pp. 989–1006, 2016.

[3] J. Akedo, "Aerosol deposition of ceramic thick films at room temperature: densification mechanism of ceramic layers," *Journal of the American Ceramic Society*, vol. 89, no. 6, pp. 1834–1839, 2006.

[4] A. Papyrin, V. Kosarev, S. Klinkov, A. Alkhimov, and V. M. Fomin, *Cold spray technology*. Elsevier, 2006.

[5] S. G. Bierschenk, M. F. Becker, and D. Kovar, "Gas and ceramic particle velocities for micro-cold spray," *Journal of Aerosol Science*, vol. 169, p. 106113, 2023.

[6] A. Alhijaily, Z. M. Kilic, and A. P. Bartolo, "Teams of robots in additive manufacturing: a review," *Virtual and Physical Prototyping*, vol. 18, no. 1, p. e2162929, 2023.

[7] R. F. Stone, W. Zhou, E. Akleman, V. R. Krishnamurthy, and Z. Sha, "Print as a dance duet: Communication strategies for collision-free arm-arm coordination in cooperative 3d

printing," in *International Design Engineering Technical Conferences and Computers and Information in Engineering Conference*, vol. 87295, p. V002T02A081, American Society of Mechanical Engineers, 2023.

[8] J. P. Wachsmuth, *Multiple independent extrusion heads for fused deposition modeling*. PhD thesis, Virginia Tech, 2008.

[9] L. Poudel, L. G. Marques, R. A. Williams, Z. Hyden, P. Guerra, O. L. Fowler, Z. Sha, and W. Zhou, "Toward swarm manufacturing: architecting a cooperative 3d printing system," *Journal of Manufacturing Science and Engineering*, vol. 144, no. 8, p. 081004, 2022.

[10] J. Akedo, "Aerosol deposition method for fabrication of nano crystal ceramic layer," in *Materials Science Forum*, vol. 449, pp. 43–48, Trans Tech Publ, 2004.

[11] H. Bui, H. A. Pierson, S. N. Pinkley, and K. M. Sullivan, "Toolpath planning for multi-gantry additive manufacturing," *IISE Transactions*, vol. 53, no. 5, pp. 552–567, 2021.

[12] F. Fenollosa, J. R. Gomà, I. Buj-Corral, A. T. Otero, J. Minguella-Canela, R. Uceda, A. Valls, and M. Ayats, "Foreseeing new multi-material fff-additive manufacturing concepts meeting mimicking requirements with living tissues," *Procedia Manufacturing*, vol. 41, pp. 1063–1070, 2019.

[13] J. Zhang and B. Khoshnevis, "Optimal machine operation planning for construction by contour crafting," *Automation in Construction*, vol. 29, pp. 50–67, 2013.

[14] A. Alhijaily, Z. M. Kilic, and P. Bartolo, "Development of a novel gantry system for cooperative printing of plastic materials," *Virtual and Physical Prototyping*, vol. 19, no. 1, p. e2305208, 2024.

[15] D. Hanft, J. Exner, M. Schubert, T. Stöcker, P. Fuierer, and R. Moos, "An overview of the aerosol deposition method: Process fundamentals and new trends in materials applications," *J. Ceram. Sci. Technol*, vol. 6, no. 3, pp. 147–182, 2015.

[16] L. Dongwong and S. Nam, "Factors affecting surface roughness of al2o3 films deposited on cu substrates by an aerosol deposition method," *Journal of Ceramic Processing Research*, vol. 11, no. 1, pp. 100–106, 2010.

[17] D.-W. Lee, H.-J. Kim, Y.-H. Kim, Y.-H. Yun, and S.-M. Nam, "Growth process of α-al2o3 ceramic films on metal substrates fabricated at room temperature by aerosol deposition," *Journal of the American Ceramic Society*, vol. 94, no. 9, pp. 3131–3138, 2011.

[18] J. Akedo, "Room temperature impact consolidation (rtic) of fine ceramic powder by aerosol deposition method and applications to microdevices," *Journal of Thermal Spray Technology*, vol. 17, pp. 181–198, 2008.

[19] M. A. Piechowiak, J. Henon, O. Durand-Panteix, G. Etchegoyen, V. Coudert, P. Marchet, and F. Rossignol, "Growth of dense ti3sic2 max phase films elaborated at room temperature by aerosol deposition method," *Journal of the European Ceramic Society*, vol. 34, no. 5, pp. 1063–1072, 2014.

[20] J. Henon, M. A. Piechowiak, O. Durand-Panteix, G. Etchegoyen, O. Masson, C. Dublanche-Tixier, P. Marchet, B. Lucas, and F. Rossignol, "Dense and highly textured coatings obtained by aerosol deposition method from ti3sic2 powder: Comparison to a dense material sintered by spark plasma sintering," *Journal of the European Ceramic Society*, vol. 35, no. 4, pp. 1179–1189, 2015.

[21] S. G. Bierschenk, *Effect of impact angle on deposition of LiNbO□ films by micro-cold spray*. PhD thesis, 2021.

[22] M. D. Crocker, *Influence of spray angle and carrier gas type on micro cold spray deposition of Cu coatings on AlN substrates*. PhD thesis, 2023.

[23] J. McCallister, M. Gammage, J. Keto, M. Becker, and D. Kovar, "Influence of agglomerate morphology on micro cold spray of ag nanopowders," *Journal of Aerosol Science*, vol. 151, p. 105648, 2021.